

CrossMark  
click for updatesCite this: *Chem. Sci.*, 2016, 7, 1521

# A highly active nickel electrocatalyst shows excellent selectivity for CO<sub>2</sub> reduction in acidic media†

Gaia Neri, Iain M. Aldous, James J. Walsh, Laurence J. Hardwick and Alexander J. Cowan\*

The development of selective electrocatalysts for CO<sub>2</sub> reduction in water offers a sustainable route to carbon based fuels and feedstocks. However, molecular catalysts are typically studied in non-aqueous solvents, in part to avoid competitive H<sub>2</sub> evolution. [Ni(cyclam)]<sup>2+</sup> (**1**) is one of the few known electrocatalysts that operate in water and 30 years after its report its activity remains a rarely surpassed benchmark. Here we report that [Ni(cyclam-CO<sub>2</sub>H)]<sup>2+</sup> (cyclam-CO<sub>2</sub>H = 1,4,8,11-tetraazacyclotetradecane-6-carboxylic acid (**2**)) shows greatly enhanced activity *versus* **1** for CO production. At pHs < pK<sub>a</sub> of the pendant carboxylic acid a large increase in catalytic activity occurs. Remarkably, despite the high proton concentration (pH 2), **2** maintains selectivity for CO<sub>2</sub> reduction and is believed to be unique in operating selectively in such acidic aqueous solutions.

Received 1st September 2015  
Accepted 20th November 2015

DOI: 10.1039/c5sc03225c

www.rsc.org/chemicalscience

## Introduction

The discovery of catalysts for the conversion of carbon dioxide (CO<sub>2</sub>) into fuels and feedstocks using renewable energy resources such as solar and wind generated electrical is amongst the most significant challenges in chemical research.<sup>1</sup> Of particular interest is the reduction of CO<sub>2</sub> to carbon monoxide (CO<sub>2</sub> + 2e<sup>-</sup> + 2H<sup>+</sup> → CO + H<sub>2</sub>O  $E_{\text{ap}}^0(V_{\text{NHE}}) = -0.12 - 0.059 \text{ pH}$ )<sup>2</sup> as CO is a key industrial feedstock that can be used to generate a wide range of hydrocarbon products by Fischer-Tropsch chemistry. To enable practical utilisation, CO<sub>2</sub> reduction electrocatalysts will need to be used in tandem with a sustainable oxidation reaction, such as water splitting (H<sub>2</sub>O → 2e<sup>-</sup> + 2H<sup>+</sup> + 1/2O<sub>2</sub>,  $E_{\text{ap}}^0(V_{\text{NHE}}) = 1.23 - 0.059 \text{ pH}$ ) making the development of low cost, selective CO<sub>2</sub> reduction catalysts that operate in water at a range of pHs an imperative goal. However the majority of studies to date using molecular catalysts have been carried out in aprotic solvents such as dimethylformamide (DMF) and acetonitrile (CH<sub>3</sub>CN) with Brønsted acids added. Careful control of the acid concentration, coupled to the relatively high solubility of CO<sub>2</sub> in these solvents minimises competitive H<sub>2</sub> production (2H<sup>+</sup> + 2e<sup>-</sup> → H<sub>2</sub>,  $E_{\text{ap}}^0(V_{\text{NHE}}) = 0 - 0.059 \text{ pH}$ ). A further complication is that any CO<sub>2</sub> electrolyser will require the cathode and anode to be separated by a membrane. To date the most effective membranes are proton

exchange materials<sup>3</sup> making the study of CO<sub>2</sub> reduction in acidic conditions of particular interest. [Ni(cyclam)]<sup>2+</sup> (**1**) is a low cost, highly selective CO<sub>2</sub> reduction catalyst producing solely CO in water at pHs 7–4. Since the initial reports over 30 years ago,<sup>4–6</sup> numerous attempts have been made to develop nickel cyclam catalysts with improved rate constants and onset potentials.<sup>7</sup> However to the best of our knowledge only two reports observed an increase in the catalyst performance,<sup>8,9</sup> with functionalisation of both the amines and carbon backbone typically causing losses in selectivity and excessive hydrogen production.

The mechanism for the reduction of CO<sub>2</sub> to CO by **1** has been extensively studied,<sup>5,10–13</sup> and although the exact nature of the active species has yet to be unambiguously identified, several factors have been made clear. Firstly, [Ni(cyclam)]<sup>+</sup> adsorbs on to some metal electrodes including Sn, Pb,<sup>14</sup> and Hg,<sup>5</sup> and adsorption onto the electrode is key for efficient CO<sub>2</sub> reduction.<sup>11</sup> **1** has also been shown to act as a homogeneous CO<sub>2</sub> reduction catalyst when used with a glassy carbon electrode (GCE)<sup>15</sup> however the level of activity was significantly lower than can be achieved on Hg, which in part may be due to suppression of catalyst degradation pathways on Hg.<sup>16</sup> Indeed Hg remains a common electrode for fundamental studies such as that presented here. At pH 5 adsorption initiates at potentials positive of the formal Ni<sup>II/I</sup> couple in solution (−1.3 V<sub>NHE</sub>) and a monolayer is formed at *ca.* −1 V<sub>NHE</sub>. The adsorbed Ni<sup>I</sup> complex is predicted to bind in an η<sup>1</sup>-C mode to CO<sub>2</sub>, prior to the transfer of a second electron to the catalyst centre.<sup>13</sup> Computational studies<sup>13,17,18</sup> indicate that the structure of the adsorbed complex is a *trans*-I conformation,<sup>19</sup> with the axial amine hydrogens aiding CO<sub>2</sub> binding. In solution **1** can adopt five

Department of Chemistry, Stephenson Institute for Renewable Energy, The University of Liverpool, UK. E-mail: a.j.cowan@liverpool.ac.uk

† Electronic supplementary information (ESI) available: Including full experimental details, surface coverage measurements and supporting electrochemical measurements. See DOI: 10.1039/c5sc03225c



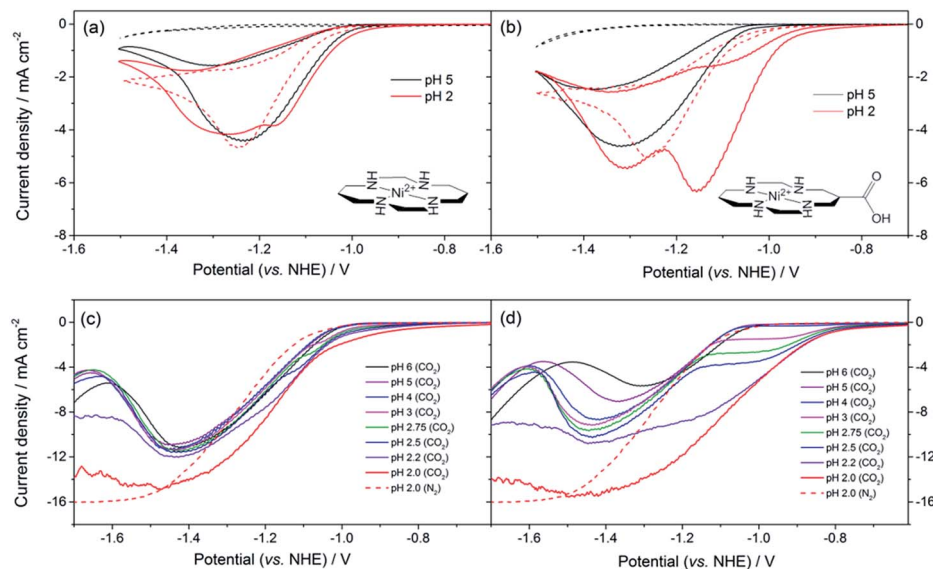


Fig. 1 CVs of (a) **1** and (b) **2** (0.1 mM) under CO<sub>2</sub> (solid lines) and Ar (dashed), at pH 5 (black) and 2 (red). Rotating disk electrode voltammetry of (c) **1** and (d) **2** (0.1 mM) under CO<sub>2</sub> (solid lines) and Ar (dashed) recorded at 800 rpm at the pH indicated. All experiments are recorded using a Hg–Au amalgam electrode in 0.1 M NaClO<sub>4</sub>.

different isomeric forms<sup>11</sup> and for clarity structures of **1** and **2** are drawn in a planar geometry (Fig. 1). Numerous studies have proposed that the decline in activity upon cyclam modification is due to conformational changes limiting the availability of the N–H group suggesting their critical role in catalysis.<sup>5,13,17</sup> Finally, **1** is most active at pH ~4–5 indicating that dissolved CO<sub>2</sub> and not HCO<sub>3</sub><sup>–</sup> or CO<sub>3</sub><sup>2–</sup> is the preferred substrate. At pH values less than 4 H<sub>2</sub> evolution dominates and CO<sub>2</sub> selectivity is lost.<sup>9</sup>

Only a limited number of other classes of molecular CO<sub>2</sub> reduction electrocatalysts for use in water are known.<sup>5,20–25</sup> Of relevance are recent studies on organic catalysts including mercaptopyridine,<sup>26</sup> an iridium pincer catalyst<sup>24</sup> and very recently a water soluble iron porphyrin catalyst, labelled WSCAT,<sup>27</sup> which preliminary data suggests is an extremely active catalyst at pH 6.7, although at lower pH values only H<sub>2</sub> was produced. The limited pH range appears to be typical of CO<sub>2</sub> reduction catalysts with most being studied between pH 6 and 7. In addition to WSCAT, Savéant *et al.*<sup>28,29</sup> have also extensively studied other iron porphyrins for use in DMF. In an important breakthrough, a large increase in electrocatalytic activity for CO<sub>2</sub> reduction to CO by an iron porphyrin modified with phenolic groups in DMF + 2.0 M H<sub>2</sub>O was reported.<sup>22</sup> The acidic phenol groups on the catalyst framework acted as both a local proton source and to aid CO<sub>2</sub> binding, greatly accelerating the proton coupled reduction of CO<sub>2</sub>, and similar approaches have now been employed by several groups studying a range of transition metal electrocatalysts for use in non-aqueous solvents.<sup>30–32</sup> While these studies show that the addition of acidic groups can greatly accelerate the rate of reduction of CO<sub>2</sub> in DMF, they have not been applied to catalysts that are active in water. Here we demonstrate that the modification of **1** with a carboxylic acid leads to a step change in catalytic activity in water with a five-fold increase in the observed rate constant

( $k_{\text{obs}}$ ), the turnover frequency per adsorbed catalyst, for **2** compared to **1**, at  $-0.99 V_{\text{NHE}}$ , near the foot of the catalytic wave. We also note an extremely high  $k_{\text{obs}} = 3.4 (\pm 1.0) \times 10^3 \text{ s}^{-1}$  at  $-1.25 V_{\text{NHE}}$ . Perhaps most remarkable is that catalyst **2** operates in acidic conditions whilst maintaining selectivity towards CO<sub>2</sub>.

## Results

The synthesis of **2**, a derivative of **1** with a carboxylate group on the carbon backbone (Fig. 1) has been reported elsewhere, where we examined the immobilisation of **2** on metal oxide surfaces for the development of a photocatalytic system.<sup>33</sup> Cyclic voltammograms (CVs) of **1** and **2** on a Hg/Au electrode at pH 5, higher than the pK<sub>a</sub> of the carboxylic acid group of **2** are in line with past reports, Fig. 1a and b. A Ni<sup>III/I</sup> couple is present under argon at  $-1.30 V_{\text{NHE}}$  (**1**) and  $-1.33 V_{\text{NHE}}$  (**2**), (see Fig. S1† for an expansion). Under CO<sub>2</sub> a large current enhancement, of similar magnitude for both **2** and **1** indicates that catalytic CO<sub>2</sub> reduction is occurring.<sup>4,33</sup> At pH 2 under argon the Ni<sup>III/I</sup> couples of both **1** and **2** are no longer visible by CV, and a catalytic curve due to proton reduction at potentials negative of  $-1.1 V_{\text{NHE}}$  is observed, Fig. 1a and b. The addition of CO<sub>2</sub> to **1** at pH 2 leads to only a slight increase in current density, indicating that some CO<sub>2</sub> reduction may occur at this pH (Fig. 1a), although we show below that H<sub>2</sub> evolution dominates. In contrast, the current density of **2** under CO<sub>2</sub> is notably increased and shifted anodic of the current response under argon (Fig. 1b, pH 2) indicating that **2** is an extremely active catalyst for CO<sub>2</sub> reduction even at very low pHs.

Bulk electrolysis experiments (Fig. S7†) confirm that **2** remains selective towards CO production at pH 2 and that its activity exceeds that of the parent catalyst **1**.  $5.2 \pm 0.3 \text{ C}$  of charge is passed within 1 hour during the electrolysis of an



unstirred solution (3  $\mu\text{M}$ ) of **2** at  $-0.99 V_{\text{NHE}}$  with a very good selectivity towards CO production  $>4 : 1 \text{ CO} : \text{H}_2$  (faradaic efficiency (FE), total = 81%,  $\text{H}_2 = 15 \pm 5\%$ ,  $\text{CO} = 66 \pm 9\%$ , with errors being the result of 3 experiments). This corresponds to an average bulk turnover number of 591 for CO in 1 hour. In contrast **1** passes only  $2.0 \pm 0.2\text{C}$  in 1 hour with a lower selectivity  $0.2 : 1 \text{ CO} : \text{H}_2$  (FE, total = 86%,  $\text{H}_2 = 73 \pm 16\%$ ,  $\text{CO} = 13 \pm 10\%$ ), and a bulk turnover number of *ca.* 45 for CO production. No liquid phase products were detected by NMR.  $[\text{Ni}(\text{cyclam})]^{2+}$  and its derivatives are known to form inactive species in the presence of  $\text{CO}$ ,<sup>34</sup> however activity can be maintained through constant  $\text{CO}_2$  purging and experiments with **2** over a 7.5 hour period show activity being maintained, Fig. S8.†

To understand the factors behind the enhanced activity of **2** at low pH we have examined the electrochemical response of **1** and **2** over a wide pH (6–2) range using rotating disc electrode (RDE) voltammetry, (Fig. 1c and d), differential pulse voltammetry (DPV, Fig. S2 and S3†) and CV measurements (Fig. S4–6†). RDE measurements are employed to study the catalysis under  $\text{CO}_2$  as they minimise the effects of substrate diffusion and product inhibition, simplifying the analysis of the electrochemical response. Between pHs 6 and 4 RDE measurements of **2** under  $\text{CO}_2$  show only a slight increase in plateau current density, Fig. 1d. Between pH 3 and 2 a dramatic change is noted with a new reductive feature (*ca.*  $-0.95 \text{ V}$ ) growing in under  $\text{CO}_2$  as the pH decreases, which is shown above to be due to catalytic  $\text{CO}_2$  reduction. This leads to a large decrease in the potential necessary for catalysis between pH 5 and 2 of *ca.* 240 mV *versus* the normal hydrogen electrode. In the RDE measurements we define the potential necessary for catalysis as being when the current density exceeds  $2 \text{ mA cm}^{-2}$ .<sup>35</sup> In contrast with **1** we only measure a very small shift (*ca.* 50 mV) in the potential necessary for catalysis between pH 6 and 2, which will be at least in part due to the increased level of  $\text{H}_2$  production at low pHs. By pH 2 there is minimal separation of the RDE curves of **1** in the presence and absence of  $\text{CO}_2$ , Fig. 1c. This step change in behaviour of **2** but not **1** is indicative of a change in catalytic

mechanism for **2** between pH 3 and 2. Furthermore whilst the variation in overpotential for  $\text{CO}_2$  reduction brought about by a change in pH (0.18 V) is equivalent for both catalysts only **2** shows a significant change in potential necessary for catalysis. The lack of a pH dependence for **1** is further explored in the ESI (Fig. S2 and S3†) where we demonstrate that the  $\text{Ni}^{\text{II/I}}$  couple under argon is independent of pH.

In order to assess if the change in current density under  $\text{CO}_2$  with pH is due to the protonation of the carboxylic acid of **2** we have measured the  $\text{p}K_{\text{a}}$  of this group by Fourier-Transform Infrared (FTIR) spectroscopy in solution (Fig. S9†). The spectra were recorded in a 0.1 mm path length  $\text{CaF}_2$  IR cell. The initially synthesised catalyst is prepared in basic conditions and the carboxylate has  $\nu_{\text{as}}(\text{CO}_2^-)$  at  $1575 \text{ cm}^{-1}$  and  $\nu_{\text{s}}(\text{CO}_2^-)$  modes at  $1375 \text{ cm}^{-1}$  in line with literature reports for similar complexes.<sup>36</sup> Titration of a 0.1 M solution of **2** in  $\text{D}_2\text{O}$  (initial  $\text{pD} = 9.61$ ) with DCl showed the clear emergence of the carboxylic acid form of **2** with  $\nu_{\text{as}}(\text{CO})$  at  $1706 \text{ cm}^{-1}$  in  $\text{D}_2\text{O}$ , with  $\text{p}K_{\text{a}} \sim 2.6$ . Deuterated solvents are required to avoid the  $\delta(\text{HOH})$  mode of  $\text{H}_2\text{O}$  masking the spectral window of interest. There is an excellent correlation between the relative concentration of the protonated carboxylic acid in solution and the current density for **2** measured under  $\text{CO}_2$  using RDE at  $-0.99 V_{\text{NHE}}$  (Fig. 2b) and  $-1.1 V_{\text{NHE}}$  (Fig. S10†). This clearly shows that the enhancement in catalytic activity towards  $\text{CO}_2$  reduction is due to the availability of the protonated carboxylic acid group of **2** at low pH values. In contrast a similar pH titration of catalyst **1** shows no clear changes in the spectral and pH region studied.

It has been shown that for **1** the active  $\text{CO}_2$  reduction catalyst is adsorbed onto Hg electrodes.<sup>11</sup> It is therefore important to ascertain if the active form of **2** is also an adsorbed species. The current density under  $\text{CO}_2$  of **2** on a GCE is found to be significantly lower than that measured on a HMDE (Fig. S11 and S12†) suggesting that the active catalyst is indeed surface adsorbed **2**. The surface concentration of **2** on the HMDE electrode has been measured using double-potential-step chronocoulometry<sup>11</sup> (Tables S1–S3†) and is found to be  $2.0 (\pm 0.2) \times$

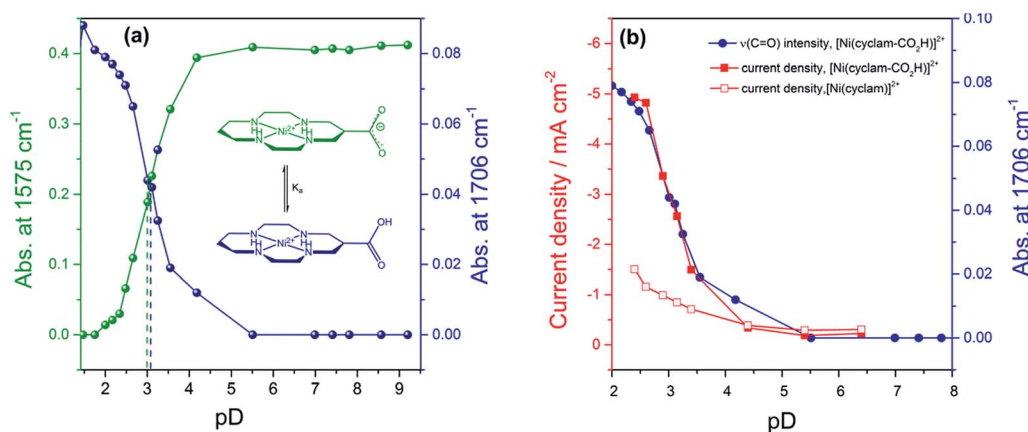


Fig. 2 (a) pD titration curves obtained by plotting the IR intensity of the peaks of the carboxylic acid ( $1706 \text{ cm}^{-1}$ , blue) and carboxylate ( $1575 \text{ cm}^{-1}$ , green). (b) Relationship between  $\text{CO}_2$  reduction current measured at  $-0.99 V_{\text{NHE}}$  of **2** (filled squares) by rotating disk electrode voltammetry (800 rpm,  $100 \text{ mV s}^{-1}$ ), relative concentration of carboxylic acid (given by the  $\nu_{\text{as}}(\text{CO})$  at  $1706 \text{ cm}^{-1}$ , blue circles) and pD. The current density of **1** under  $\text{CO}_2$  with pH is also shown (open squares).  $\text{pD} = \text{pH} + 0.4$ .



$10^{-10}$  mol cm $^{-2}$  at  $-0.99$  V $_{\text{NHE}}$  at pH 5, similar to that previously reported for **1**,  $1.6 (\pm 0.2) \times 10^{-10}$  mol cm $^{-2}$ .<sup>34</sup> At pH 2 the surface concentration of both **1** and **2** are changed by a minimal amount ( $2.2 (\pm 0.2) \times 10^{-10}$  mol cm $^{-2}$  and  $1.6 (\pm 0.2) \times 10^{-10}$  mol cm $^{-2}$  respectively at  $-0.99$  V $_{\text{NHE}}$ ), indicating that the large increase in activity of **2** cannot be attributed to a change in the surface coverage of the catalyst with pH.

The kinetic behaviour of **1** and **2** at pH 2 can be obtained from the RDE measurements carried out at different rotation rates (Fig. S15 $\dagger$ ). We calculate the kinetic activity of the catalyst from voltammetric sweep measurements as it has recently been highlighted that turnover frequencies obtained from long-term bulk electrolysis measurements at high current densities can be complicated by a range of factors including (i) substrate diffusion, (ii) product inhibition and (iii) catalyst deactivation.<sup>37</sup>

Using the limiting current obtained from the intercepts of Koutecký–Levich plots (Fig. S14 and S15 $\dagger$ ) we can obtain an apparent first order rate constant ( $k_{\text{obs}}$ , s $^{-1}$ ), *i.e.* the turnover frequency (TOF) per adsorbed catalyst using eqn (1).<sup>38</sup>

$$i_{\text{cat}} = nF\Gamma A k_{\text{obs}} \quad (1)$$

where  $n$  is the number of electrons transferred (2),  $\Gamma$  the surface coverage (mol cm $^{-2}$ ) and  $A$  the electrode area (cm $^2$ ). We obtain  $k_{\text{obs}}$  values of  $3.5 (\pm 1.0) \times 10^1$  s $^{-1}$  and  $1.9 (\pm 0.2) \times 10^2$  s $^{-1}$  for **1** and **2** respectively at pH 2,  $-0.99$  V $_{\text{NHE}}$ . It is apparent that at pH 2 complex **2** turns over approximately five times faster than **1** at  $-0.99$  V $_{\text{NHE}}$  and the activity of **2** exceeds **1** at all potentials examined, Table S4. $\dagger$  It should also be noted that **1** primarily produces H $_2$  in bulk electrolysis experiments therefore the measured  $k_{\text{obs}}$  for **1** at pH 2 under CO $_2$  is expected to have a significant contribution from proton reduction. In contrast **2** is shown to be selective towards CO $_2$  and at potentials positive of  $-1.3$  V $_{\text{NHE}}$  there is a large difference in  $k_{\text{obs}}$  obtained in the presence and absence of the substrate (CO $_2$ ), Fig. 3, Table S4. $\dagger$  At potentials corresponding to the plateau current,  $-1.25$  V $_{\text{NHE}}$ , we calculate a very large rate constant under CO $_2$ ,  $k_{\text{obs}} = 3.4$

( $\pm 1.0$ )  $\times 10^3$  s $^{-1}$  compared to only  $k_{\text{obs}} = 3.3 (\pm 0.4) \times 10^2$  s $^{-1}$  under N $_2$ . This kinetic control between proton and CO $_2$  reduction offers a rationalisation of the very high selectivity of **2** even in the presence of a high proton concentration.

## Discussion

Comparison of the catalyst performance with existing benchmarks is ideally carried out by comparison of the overpotential dependence of the catalytic rate constant.<sup>1</sup> Although these data are becoming increasingly reported for catalysts in aprotic solvents, we are unaware of its availability for the few CO $_2$  reduction catalysts that operate in water.<sup>27</sup> The value of  $k_{\text{obs}} = 3.4 (\pm 1.0) \times 10^3$  s $^{-1}$  for **2** at pH 2 under CO $_2$ , measured at a single potential ( $-1.25$  V $_{\text{NHE}}$ ) exceeds the reported TOF of the majority of known water soluble CO $_2$  reduction catalysts,<sup>9,24,34</sup> including **1** ( $6.3 \times 10^1$  s $^{-1}$ ).<sup>34</sup> To the best of our knowledge there has only been one reported water soluble catalyst that operates at a greater rate, the recently reported iron porphyrin catalyst WSCAT.<sup>27</sup> We also note that the measured rate constant for **2** under CO $_2$  also exceeds that of many of the most commonly studied CO $_2$  reduction catalysts operating in aprotic solvents,<sup>1</sup> which is perhaps surprising given the significantly lower dissolved CO $_2$  concentration in water (0.28 M (CH $_3$ CN), 34 mM (H $_2$ O)).

However the most significant feature of **2** is its selectivity towards CO $_2$  even under acidic conditions. All previously reported derivatives of **1** have shown predominantly hydrogen production outside of a small pH window<sup>7,11</sup> and we note that the majority of CO $_2$  reduction catalysts are reported at pHs close to neutral (5–7),<sup>24,25,27</sup> making the ability of **2** to operate at pHs as low as 2 unusual. The correlation between the current density under CO $_2$  and the protonation state of the carboxylic acid group of **2** suggests that the protonation state of the catalyst is an important factor in the enhanced TOF, and hence selectivity towards CO $_2$  of **2** in acidic solutions (Fig. 2b). It may be envisaged that protonation of the carboxylic acid group leads to **2** being more readily reduced to form the active Ni $^{\text{I}}$  catalyst, however DPV studies indicate the Ni $^{\text{II/I}}$  couple to be pH independent under argon, Fig. S2 and 3. $\dagger$  Alternatively previous studies have shown that the presence of a local proton source can accelerate CO $_2$  reduction and it is viable that the acid group may also aid catalysis here.<sup>28,30–32</sup> In the homogenous reduction of CO $_2$  by **1** in acetonitrile a proton concentration dependent peak in the CV, similar to the feature observed by RDE (Fig. 1d) here at *ca.*  $-0.95$  V $_{\text{NHE}}$  was reported.<sup>16</sup> This peak was assigned to the reduction of a protonated CO $_2$  adduct, with this proton dependent electron transfer becoming the rate limiting step in CO $_2$  catalysis under certain conditions. It is feasible that the protonated carboxylic acid is acting as local proton source during the reduction of a CO $_2$  adduct here. Such an interaction is geometrically feasible. The cobalt analogue of **2** has been reported for use in dye-sensitized solar cells with binding of the  $-\text{CO}_2\text{H}$  group directly to the metal centre.<sup>36,39</sup> However we do recognise that the empirical nature of the relationship in Fig. 2b does not provide direct evidence of the functional role of the carboxylic acid. We are currently also unable to discount the

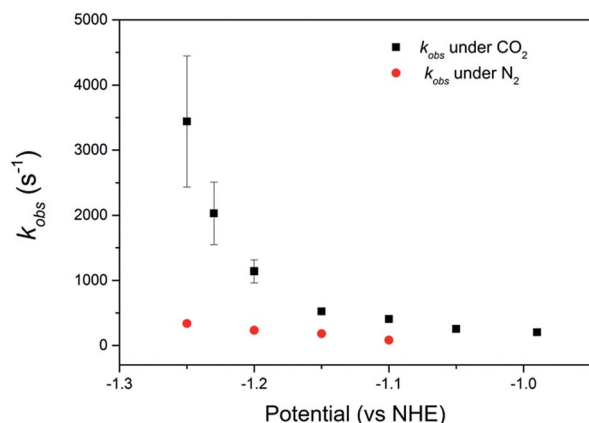


Fig. 3 Plot of  $k_{\text{obs}}$  of catalyst **2**, calculated from the intercepts of Koutecký–Levich plots, vs. potential at pH 2. Values are obtained averaged from 3 independent measurements with the error bars calculated from the uncertainties in the intercepts of the Koutecký–Levich plots.



role of other potential mechanistic aspects including a possible change in structure of the adsorbed catalyst or change in the catalysts CO<sub>2</sub> affinity and further mechanistic studies are currently underway.

The enhanced activity of **2** and the ability to maintain selectivity towards CO<sub>2</sub> across a wide pH range are highly desirable traits. It is likely that robustness towards local pH fluctuations and the ability to be employed in electrolyzers using proton exchange membranes will be advantageous for any practically applicable catalyst. However operating at pH 2 does have implications regarding the overpotential for catalysis. The potential necessary for catalysis with a current density of 2 mA cm<sup>-2</sup> in Fig. 1 is ca. -0.9 V<sub>NHE</sub>, corresponding to an overpotential of ca. -0.65 V versus the apparent equilibrium potential for CO<sub>2</sub> reduction to CO at pH 2. Whilst not dissimilar to other previous studies in aqueous solutions,<sup>9,27</sup> it is significantly higher than typically required in solvents such as DMF, CH<sub>3</sub>CN and ionic liquids indicating that further improvements in molecular catalysts for use in aqueous solutions are still required.

## Conclusions

The development of selective and efficient molecular catalysts for electrocatalytic CO<sub>2</sub> reduction in water is amongst the most challenging goals for the chemistry community. Complex **2** is based on a low cost metal centre and is able to use a pendant acid group to achieve excellent selectivity and activity towards CO<sub>2</sub> even at the very low pH value of 2. The activity of **2** greatly exceeds the parent complex (**1**) under identical conditions, something that has been rarely achieved in over 30 years of research. **2** is also found to have be amongst the most active aqueous CO<sub>2</sub> reduction catalysts and we believe that these characteristics make it of great significance to the field of electrocatalytic CO<sub>2</sub> reduction.

## Acknowledgements

AJC, JJW (EP/K006851/1) and LJH, IMA (EP/K006835/1) acknowledge the EPSRC for funding. Prof. D. Shchukin is thanked for access to the FTIR.

## Notes and references

- 1 C. Costentin, M. Robert and J.-M. Savéant, *Chem. Soc. Rev.*, 2013, **42**, 2423–2436.
- 2 In line with previous convention [1]  $E_{\text{ap}}^0$  is the apparent equilibrium potential at 25 °C, 1 atm gas pressure with 1 M solutes except for the proton concentration.
- 3 W. Li, S. W. Sheehan, D. He, Y. He, X. Yao, R. L. Grimm, G. W. Brudvig and D. Wang, *Angew. Chem., Int. Ed.*, 2015, **54**, 11428–11432.
- 4 M. Beley, J. P. Collin, R. Ruppert and J. P. Sauvage, *J. Chem. Soc., Chem. Commun.*, 1984, 1315–1316.
- 5 M. Beley, J. P. Collin, R. Ruppert and J. P. Sauvage, *J. Am. Chem. Soc.*, 1986, **108**, 7461–7467.
- 6 B. J. Fisher and R. Eisenberg, *J. Am. Chem. Soc.*, 1980, **102**, 7361–7363.
- 7 J. Qiao, Y. Liu, F. Hong and J. Zhang, *Chem. Soc. Rev.*, 2014, **43**, 631–675.
- 8 E. Fujita, J. Haff, R. Sanzenbacher and H. Elias, *Inorg. Chem.*, 1994, **33**, 4627–4628.
- 9 J. Schneider, H. Jia, K. Kobiro, D. E. Cabelli, J. T. Muckerman and E. Fujita, *Energy Environ. Sci.*, 2012, **5**, 9502–9510.
- 10 M. Fujihira, Y. Hirata and K. Suga, *J. Electroanal. Chem.*, 1990, **292**, 199–215.
- 11 G. B. Balazs and F. C. Anson, *J. Electroanal. Chem.*, 1992, **322**, 325–345.
- 12 C. A. Kelly, E. L. Blinn, N. Camaioni, M. D'Angelantonio and Q. G. Mulazzani, *Inorg. Chem.*, 1999, **38**, 1579–1584.
- 13 J. Schneider, H. Jia, J. T. Muckerman and E. Fujita, *Chem. Soc. Rev.*, 2012, **41**, 2036–2051.
- 14 P. Jacquinet and P. C. Hauser, *Electroanalysis*, 2003, **15**, 1437–1444.
- 15 J. D. Froehlich and C. P. Kubiak, *Inorg. Chem.*, 2012, **51**, 3932–3934.
- 16 J. D. Froehlich and C. P. Kubiak, *J. Am. Chem. Soc.*, 2015, **137**, 3565–3573.
- 17 S. Sakaki, *J. Am. Chem. Soc.*, 1990, **112**, 7813–7814.
- 18 K. Bujno, R. Bilewicz, L. Siegfried and T. A. Kaden, *J. Electroanal. Chem.*, 1998, **445**, 47–53.
- 19 E. J. Billo, P. J. Connolly, D. J. Sardella, J. P. Jasinski and R. J. Butcher, *Inorg. Chim. Acta*, 1995, **230**, 19–28.
- 20 P. Kang, S. Zhang, T. J. Meyer and M. Brookhart, *Angew. Chem., Int. Ed.*, 2014, **53**, 8709–8713.
- 21 T. Yoshida, K. Kamato, M. Tsukamoto, T. Iida, D. Schlettwein, D. Wöhrle and M. Kaneko, *J. Electroanal. Chem.*, 1995, **385**, 209–225.
- 22 S. Lin, C. S. Diercks, Y.-B. Zhang, N. Kornienko, E. M. Nichols, Y. Zhao, A. R. Paris, D. Kim, P. Yang, O. M. Yaghi and C. J. Chang, *Science*, 2015, **349**, 1208–1213.
- 23 E. Barton Cole, P. S. Lakkaraju, D. M. Rampulla, A. J. Morris, E. Abelev and A. B. Bocarsly, *J. Am. Chem. Soc.*, 2010, **132**, 11539–11551.
- 24 P. Kang, T. J. Meyer and M. Brookhart, *Chem. Sci.*, 2013, **4**, 3497–3502.
- 25 P. Kang, Z. Chen, A. Nayak, S. Zhang and T. J. Meyer, *Energy Environ. Sci.*, 2014, **7**, 4007–4012.
- 26 D. Xiang, D. Magana and R. B. Dyer, *J. Am. Chem. Soc.*, 2014, **136**, 14007–14010.
- 27 C. Costentin, M. Robert, J.-M. Savéant and A. Tatin, *Proc. Natl. Acad. Sci. U. S. A.*, 2015, **112**, 6882–6886.
- 28 C. Costentin, S. Drouet, M. Robert and J.-M. Savéant, *Science*, 2012, **338**, 90–94.
- 29 C. Costentin, G. Passard, M. Robert and J.-M. Savéant, *Proc. Natl. Acad. Sci. U. S. A.*, 2014, **111**, 14990–14994.
- 30 F. Franco, C. Cometto, F. Ferrero Vallana, F. Sordello, E. Priola, C. Minero, C. Nervi and R. Gobetto, *Chem. Commun.*, 2014, **50**, 14670–14673.
- 31 J. Agarwal, T. W. Shaw, H. F. Schaefer and A. B. Bocarsly, *Inorg. Chem.*, 2015, **54**, 5285–5294.



- 32 S. T. Ahn, E. A. Bielinski, E. M. Lane, Y. Chen, W. H. Bernskoetter, N. Hazari and G. T. R. Palmore, *Chem. Commun.*, 2015, **51**, 5947–5950.
- 33 G. Neri, J. J. Walsh, C. Wilson, A. Reynal, J. Y. C. Lim, X. Li, A. J. P. White, N. J. Long, J. R. Durrant and A. J. Cowan, *Phys. Chem. Chem. Phys.*, 2015, **17**, 1562–1566.
- 34 G. B. Balazs and F. C. Anson, *J. Electroanal. Chem.*, 1993, **361**, 149–157.
- 35 E. S. Rountree, B. D. McCarthy, T. T. Eisenhart and J. L. Dempsey, *Inorg. Chem.*, 2014, **53**, 9983–10002.
- 36 P. V. Bernhardt, G. K. Boschloo, F. Bozoglian, A. Hagfeldt, M. Martinez and B. Sienna, *New J. Chem.*, 2008, **32**, 705–711.
- 37 C. Costentin, S. Drouet, M. Robert and J.-M. Savéant, *J. Am. Chem. Soc.*, 2012, **134**, 11235–11242.
- 38 A. K. Vannucci, L. Alibabaei, M. D. Losego, J. J. Concepcion, B. Kalanyan, G. N. Parsons and T. J. Meyer, *Proc. Natl. Acad. Sci. U. S. A.*, 2013, **110**, 20918–20922.
- 39 G. Wei, T. W. Hambley, G. A. Lawrance and M. Maeder, *Aust. J. Chem.*, 2002, **55**, 667–673.

